ELSEVIER

Journal of Applied Geophysics 51 (2002) 63–74

JOURNAL OF APPLIED GEOPHYSICS

www.elsevier.com/locate/jappgeo

The magnetic fields of steel drums

Peter Furness*

Department of Earth Sciences, University of Queensland, St. Lucia Q4072, Australia

Received 8 February 2002; accepted 22 July 2002

Abstract

The concept of apparent susceptibility can be extended to bodies with arbitrary geometry by considering the integrated magnetization or dipole moment associated with the body. This unique characteristic can be easily computed numerically for features of arbitrary shape and susceptibility. Numerical studies reveal that the thin-walled steel drum displays an anisotropic apparent susceptibility with distinct longitudinal and transverse values. While the apparent susceptibility is independent of drum size, it varies with the susceptibility, the wall thickness and with the dimension ratio of the drum. Exact numerical modelling of total field magnetic profiles over a buried steel drum allows the evaluation of a range of approximate modelling techniques. While all reasonably match the form of the measured profile, only the response computed for an equivalent magnetic shell and that using an equivalent magnetic dipole with moment computed from the true drum susceptibilities allow the profile amplitude to be predicted with any accuracy. Of these, the latter technique is the more successful. It also provides a discernable improvement in the shape of the modelled profile.

Keywords: Environmental geophysics; Steel drums; Integral equation

1. Introduction

The magnetic method is now well established in environmental and engineering investigations for the detection of ferromagnetic constructions. Common targets of these investigations are disposal sites where waste materials are buried in steel containers. Geophysics is often required to locate these receptacles and to estimate their quantity. Magnetic surveys for this purpose must therefore be designed and the resulting data interpreted.

In order to achieve this, it is necessary to model the magnetic fields produced by thin-walled ferromagnetic containers (typically steel drums). Unfortunately, this has not been easily achieved, and two reasons for the lack of progress are easily identified.

Firstly, there is little information in the geophysical literature on the basic magnetic parameters relevant to steel containers (i.e. the susceptibility and magnetic remanence). Initial attempts at measuring susceptibilities of small samples taken from steel drums using conventional laboratory techniques by Emerson et al. (1992) and Ravat (1996) were not successful due to the effect of demagnetization. More recently, however, Eskola et al. (1999) describe a technique using a flux gate magnetometer that is suitable for the measurement of both susceptibility and remanent magnetization of thin ferromagnetic material. Unfortunately, the proper-

* Tel.: +61-0754450146; fax: +61-0754450247.
E-mail address: furness@powerup.com.au (P. Furness).

0926-9851/02/$ - see front matter © 2002 Elsevier Science B.V. All rights reserved.
PII: S0926-9851(02)00211-2

ties of only 13 samples measured by this technique are available in the literature.

It should be mentioned in this connection that some relevant information on the magnetic characteristics of steel drums has also been achieved by field measurements (Emerson et al., 1992; Ravat, 1996). By observing the magnetic responses of drums in several orientations, the effects of induced magnetization and remanence can be discriminated. These two components of the magnetization can then be found in terms of equivalent dipoles by inversion of the field data. Use of the volume of ferromagnetic material and the ambient **H** field then allows calculation of magnetizations and susceptibilities. However, while these data are useful for equivalent source modelling of the magnetic fields produced by steel drums, they do not represent the true or intrinsic parameters of the ferromagnetic material used in their construction.

The second and perhaps more significant reason for lack of progress towards a practical magnetic model for steel containers concerns the difficulty of modelling magnetic fields due to thin sheets with extreme susceptibilities. Eskola et al. (1993) have demonstrated the unsuitability of standard modelling algorithms for this purpose.

This modelling problem has prompted the use of a range of approximations for the magnetic response of steel drums. Field measurements made by Emerson et al. (1992) and Ravat (1996) have been explained in terms of equivalent dipoles or bodies of simple shape magnetized in the direction of the earth's field. However, while these techniques have been useful for predicting the shape of magnetic profiles located sufficiently remote from the drum, they fail badly to predict the amplitude.

Application of exact numerical (surface integral equation) models has similarly been less than helpful. The problem is related to the numerical instability demonstrated by many such models when applied to very thin and intensely magnetic sheets (Eskola et al., 1993; Traynin and Hansen, 1993). However, one general surface integral equation technique has been shown to be relatively robust in this regard. Recently, Furness (1999) demonstrated the ability of a general surface integral equation formulation to accommodate thin-walled ferromagnetic bodies. The technique was originally described in an electrostatic context by Phillips (1934).

It is relevant to note that two other options exist in the geophysical literature for the exact numerical modelling of drum responses. The specialized integral equation technique described by Nabigian et al. (1984) and the integrodifferential equation approach of Eskola et al. (1989) were both designed specifically to accommodate the type of thin, highly susceptible bodies of interest here.

Notwithstanding the present work employs Phillips' integral equation technique to investigate the magnetic response of a single steel drum in a nonmagnetic environment. However, since implementation of the method is quite demanding in terms of computing time and facilities, an additional emphasis in the present investigation concerns the evaluation of several approximate magnetic models for steel drums. Towards this end, advantage will take of the similarity in magnetic behaviour that exists between steel drums and spherical magnetic shells. The problem of a spherical shell exposed to a uniform magnetic field can be easily solved analytically, and the solution is readily available in the literature (e.g. Jackson, 1975). In spite of this, it apparently has not yet been used for the present purpose of modelling the magnetic fields due to thin-walled ferromagnetic containers.

2. A generalized apparent susceptibility

Previous workers in this area (e.g. Emerson et al., 1992; Ravat, 1996) have used a variety of parameters to define the magnetic characteristics of steel drums. None of these are suitable for the present study. Rather, it is convenient here to generalize the well-known concept of apparent susceptibility.

It is recalled that the apparent susceptibility is only defined for ellipsoidal bodies influenced by uniform primary fields. In this case, the magnetization is uniform and can be expressed by

$$\mathbf{M} = k\mathbf{H}$$

where k is the volume susceptibility and **H** is the local magnetic field acting inside the body. It can be expressed as the sum of the primary field and the secondary or depolarizing component due to the body itself, i.e.

$$\mathbf{H} = \mathbf{H}\mathrm{p} + \mathbf{H}_\mathrm{s}$$

The apparent susceptibility is defined so as to relate the magnetization to an axially directed primary field in the manner

$$\mathbf{M} = k_\alpha \mathbf{H}_\mathrm{p}$$

so that

$$k_\alpha = \frac{M}{H_\mathrm{p}} \tag{1}$$

However, since the magnetization is uniform, it can be expressed as

$$\mathbf{M} = \frac{\mathbf{m}}{V}$$

where V is the volume of the ellipsoid and m is the total dipole moment. Using this result, the apparent susceptibility of Eq. (1) can be alternatively expressed as

$$k_\alpha = \frac{m}{H_\mathrm{p} V} \tag{2}$$

Eq. (1) is the conventional definition of apparent susceptibility but is clearly restricted to the case of uniform magnetization associated with ellipsoidal bodies. The more general form of Eq. (2) also accommodates non-uniform magnetization associated with a body of arbitrary shape influenced by a uniform primary field. The resulting apparent susceptibility is similar to the susceptibility derived from drum rotation experiments by Emerson et al. (1992). However, there is one significant difference. These authors appear to have deduced the dipole moment by a data fitting technique from the measured magnetic response of a drum. Consequently, the dipole moment is an equivalent dipole moment and includes the effect of higher multipoles in the body's response. It is not the unique intrinsic dipole moment associated with the body. In theory, this is only derivable from the drum's observed response when measurements are made at an infinitely remote location where the influence of higher multipoles is negligible.

3. The spherical shell

The spherical shell influenced by a uniform magnetic field provides a convenient analytical model for the behaviour of thin-walled ferromagnetic containers

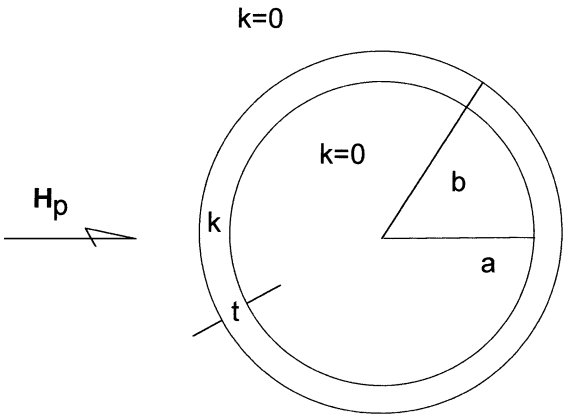

Fig. 1. Spherical shell with susceptibility k located in free space and influenced by a uniform primary magnetic field H_p.

with approximately equidimensional form. Fig. 1 shows a sectional view of a spherical shell with internal and external radii a and b, respectively. The shell with susceptibility k and thickness t is enclosed in free space and is influenced by a uniform primary magnetic field $\mathbf{H}_\mathrm{p}$.

Jackson (1975) shows that the effect of the shell in the external region is equivalent to that of a dipole with moment

$$\mathbf{m} = \frac{4\pi(b^3 - a^3)k(2k+3)}{(2k+3)(k+3) - 2k^2(a/b)^3}\mathbf{H}_\mathrm{p} \tag{3}$$

located at the center of the sphere. Internally, the shell produces a uniform magnetic field parallel to the primary field, but this is of no significance to the present discussion. An analysis of the last equation shows that for significantly thin and susceptible shells, where $k \gg 1$ and $t \ll b$, the dipole moment behaves in the manner

$$\mathbf{m} \rightarrow 2ktA\mathbf{H}_\mathrm{p}/3$$

where A is the surface area. In this case, therefore, the magnetic field produced by a thin spherical shell can be expected to depend on the product of the wall thickness, the susceptibility, the surface area and, of course, the primary field.

Substitution of Eq. (3) in Eq. (2) yields the apparent susceptibility

$$k_\alpha = \frac{3k(2k+3)}{(2k+3)(k+3) - 2k^2(a/b)^3} \tag{4}$$

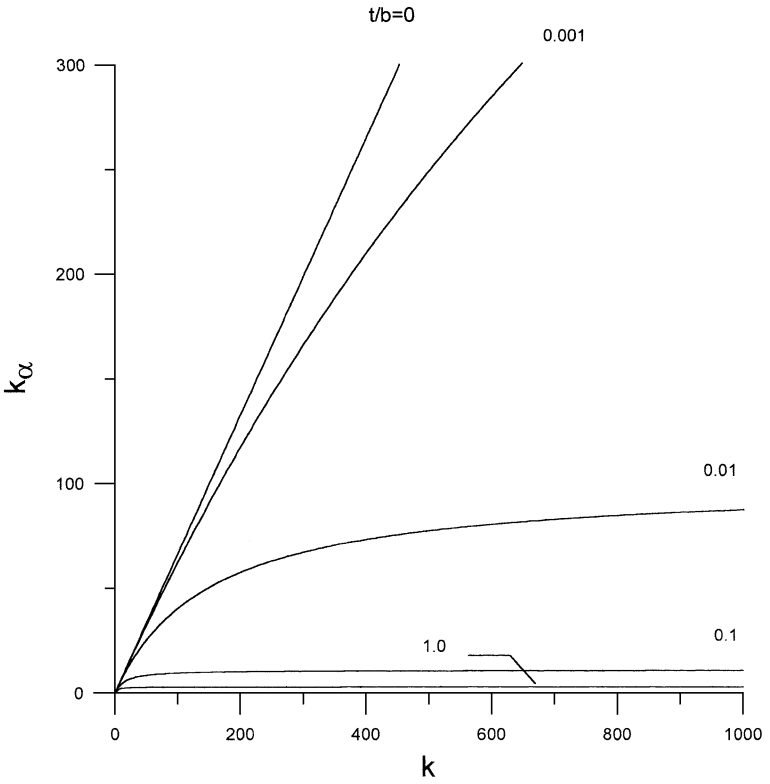

Fig. 2. Apparent susceptibility of a spherical shell with variable wall thickness as a function of susceptibility.

which is clearly independent of the size of the body. It depends on the wall thickness in terms of the ratio of radii a/b, however, for $k \gg 1$ and $t \ll b$, it can be shown to behave as

$$k_\alpha \rightarrow 2k/3$$

Fig. 2 shows the variation of the apparent susceptibility with intrinsic susceptibility for the complete range of shell thickness from $t=0$ (spherical lamina) to $t=b$ (solid sphere). The figure demonstrates that for thick shells, the magnetization is strongly reduced by the influence of a large demagnetizing field. The effect of the demagnetization is seen to diminish with decreasing wall thickness. For very thin shells, this influence is greatly reduced until in the limit as $t \rightarrow 0$; the apparent susceptibility behaves as $2k/3$ for $k \gg 1$. This reflects a dramatic improvement in the thin-walled sphere's ability to produce magnetization compared to that of thicker shells. Put differently, for most shells, the apparent susceptibility is determined by the geometry of the body through the influence of the depolarizing field. For very thin shells, however, it is largely determined by the susceptibility.

4. Modelling drum responses

The present investigation employs an integral equation model described in a magnetic context by Furness (1999). The physical situation is illustrated in Fig. 3. It shows a magnetic body with uniform susceptibility k located in free space and influenced by a primary magnetic field $\mathbf{H}_p$.

The secondary potential in the region outside the body can be expressed by

$$\phi_s(\mathbf{r}) = -\frac{k}{4\pi} \oiint_S \phi(\mathbf{r}')\hat{\mathbf{n}} \cdot \nabla' \frac{1}{|\mathbf{r}-\mathbf{r}'|} \mathrm{d}s' \qquad (5)$$

and the secondary magnetic $\mathbf{H}$ field by

$$\mathbf{H}_s(\mathbf{r}) = \frac{k}{4\pi} \nabla \oiint_S \phi(\mathbf{r}')\hat{\mathbf{n}} \cdot \nabla' \frac{1}{|\mathbf{r}-\mathbf{r}'|} \mathrm{d}s' \qquad (6)$$

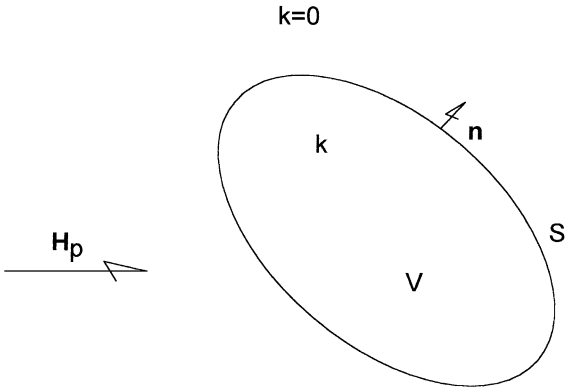

Fig. 3. Body with susceptibility k located in free space and influenced by a uniform primary magnetic field H_p.

where ϕ is the potential on the surface of the body found by solving the integral equation

$$\phi(\mathbf{r}) = \frac{2}{k+2}\phi_p(r) - \frac{k}{2\pi(k+2)} \oiint_{S'} \phi(\mathbf{r}')\hat{\mathbf{n}} \cdot \nabla' \frac{1}{|\mathbf{r}-\mathbf{r}'|} ds' \quad (7)$$

Here, S' denotes the surface of the body minus the singular point at r.

This formulation can be easily used to find the total dipole moment associated with the body (Van Bladel, 1985). This is achieved by noting that in the limit as $|\mathbf{r}-\mathbf{r}'| \to \infty$; Eq. (5) expressing the secondary potential in the external region may be written in the form

$$\phi_s(\mathbf{r}) = -\frac{k}{4\pi} \oiint_S \phi(\mathbf{r}')\hat{\mathbf{n}} ds' \cdot \nabla' \frac{1}{|\mathbf{r}-\mathbf{r}'|}$$

or

$$\phi_s(\mathbf{r}) = \frac{1}{4\pi}\mathbf{m}(\mathbf{r}') \cdot \nabla' \frac{1}{|\mathbf{r}-\mathbf{r}'|}$$

where m is the total dipole moment associated with the body given by

$$\mathbf{m} = -k \oiint_S \phi(\mathbf{r}')\hat{\mathbf{n}} ds' \quad (8)$$

The appearance of this equation can be made more familiar by the application of a well-known corollary of the divergence theorem to yield

$$\mathbf{m} = -k \int_V \int \int \nabla\phi(\mathbf{r}') dv'$$

or

$$\mathbf{m} = \int_V \int \int \mathbf{M}(\mathbf{r}') dv'$$

The above discussion has not mentioned remanent magnetization in the body. However, Eskola (1992) has noted that the influence of a uniform remanent magnetization $\mathbf{R}$ in a body of constant susceptibility k enclosed in free space is equivalent to the effect of a primary field given by $\mathbf{R}/k$ acting in the absence of remanence. It follows from the linearity of the magnetic problem in terms of the primary field that the effect of remanence in the present model can be found by employing a modified primary magnetic field given by

$$\mathbf{H}_p' = \mathbf{H}_p + \mathbf{R}/k$$

in the above equations.

5. The standard steel drum

A survey of industrial containers currently manufactured in Australia suggests that a typical 205-l closed head drum has an internal diameter of 571.5 mm, an internal height of 847 mm and a wall thickness of between 0.7 and 1.4 mm. Internal dimensions are quoted here since they do not include the effect of irregularities such as welds, seams, etc., and so more faithfully reflect the geometry of the drum walls.

There is relatively little reliable information available in the geophysical literature on the magnetic properties of the metal sheet used in the fabrication of steel drums. However, recently, Eskola et al. (1999) measured susceptibilities in the range 200–500 SI accompanying remanent magnetizations of 1000–20 000 A/m for 13 samples with thicknesses from 0.5 to 1.0 mm taken from steel sheets and drums.

On the basis of the above information, a standard drum is defined for the present investigation to have an external radius of 286.75 mm and an external height of 849 mm. The walls are assumed to be 1.0 mm thick and of material with an intrinsic susceptibility of 350 SI. Remanent magnetization is assumed to be of negligible significance compared to induced magnetization.

In the following discussion, reference to a standard drum will imply use of the above parameters. However, it will also be necessary to consider steel drums in which one or more of the parameters are different

from their standard values. These containers will also be referred to as standard drums but with an appropriate indication of the nonstandard parameter values.

The neglect of remanence in the definition of the standard drum requires some comment. There is presently no clear consensus on the importance of remanent magnetization in steel drums. Emerson et al. (1992) noted a relatively minor contribution of remanence to the observed magnetic responses in their experiments with steel drums. They argue for the likelihood of destructive interference of the magnetic fields due to remanent magnetization in the individual parts of containers fabricated from discrete components. Ravat (1996) also concluded that remanence was of significantly less importance than induced magnetization in samples taken from eight drums. On the other hand, Barrows and Rocchio (1990) reported a comparable contribution from remanent and induced magnetizations in two steel drums tested. In addition, the results of Eskola et al. (1999) show significant remanence albeit in a minority of the steel samples tested.

It is relevant to mention that the above results probably include the contribution of viscous remanent magnetization in the remanence measurements. In the present application, where interest focuses on the magnetic response of steel containers that have long been undisturbed, the influence of viscous remanence is probably best accommodated in the susceptibility parameter. This would have the result of increasing the magnitude of the susceptibilities at the expense of the measured remanent magnetizations.

Finally, it must be conceded that the neglect of remanent magnetization in the present study is as much prompted by practicality as by any other consideration. Since it is likely that remanent magnetization is acquired prior to the fabrication of steel drums, there is no simple formula for its distribution in a completed drum. While the accommodation of an arbitrary distribution of remanence in the numerical model of steel drums offers no serious challenge, a more practical technique may be to model the net remanent magnetization in the drum as a whole by the use of a modified primary magnetic field as described above.

The numerical technique described in the previous section has been used to compute the apparent susceptibility of a standard steel drum with susceptibilities in the range from 0 to 1000 units SI influenced by a uniform magnetic field in the longitudinal and transverse directions. For this purpose, the drum was represented by a polyhedron in the form of a hollow circular prism with 1440 quadrilateral faces having a maximum dimension of approximately 60 mm. Fig. 4 shows a perspective view of the outer surface of the body comprising 720 facets. The inner surface is similarly represented by 720 faces.

The results of these calculations are shown in Fig. 5 plotted against the susceptibility of the wall material. The computed apparent susceptibilities are plotted as crosses and are shown to be well fitted by an equation (shown as a continuous line) of the form

$$k_\alpha = \frac{ak}{1+bk} \tag{9}$$

where $a = 0.740176$, $b = 0.00157453$ for the longitudinal apparent susceptibility and $a = 0.627583$,

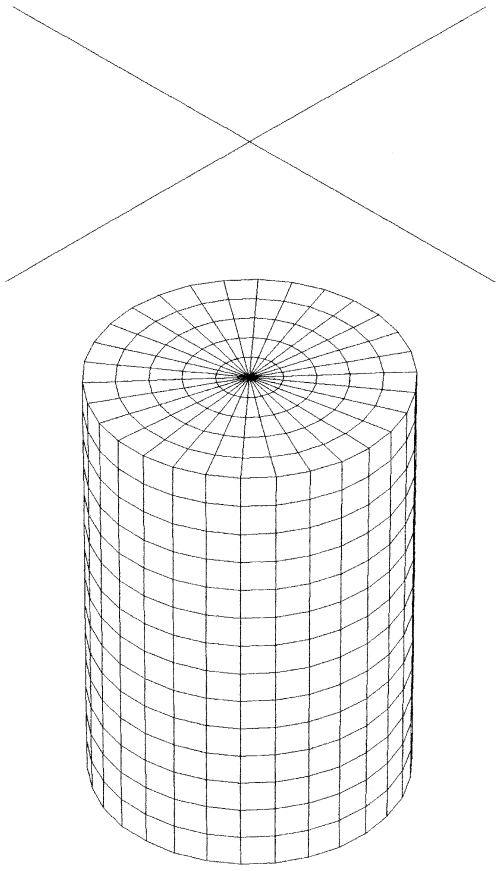

Fig. 4. Perspective view of a standard drum modelled by 720 external and 720 internal planar quadrilateral surface elements.

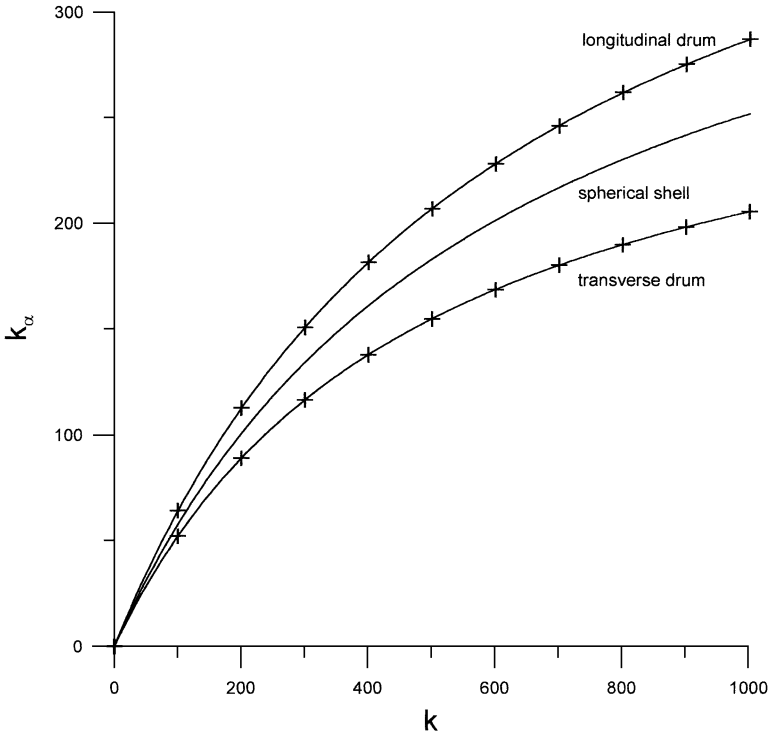

Fig. 5. Apparent susceptibility as a function of susceptibility for a standard drum influenced by a longitudinal magnetic field, a standard drum influenced by a transverse magnetic field and an equivalent spherical shell.

$b = 0.00205086$ for the transverse case. The form of this relationship is prompted by the behaviour of the apparent susceptibility in ellipsoidal bodies and has been used previously by Eskola et al. (1999).

Also included in the figure is the analytically derived curve for a thin spherical shell with equal surface area and wall thickness to the standard drum (amounting to an equal volume of ferromagnetic material). The behaviour of the longitudinal and transverse susceptibilities of the drum is seen to show the same general trend as the apparent susceptibility of the equivalent spherical shell. Interestingly, the susceptibility of the spherical shell takes on a median value between those of the drum in its two principal orientations.

The main feature of Fig. 5 is the significantly anisotropic nature of the apparent susceptibility displayed by steel drums as compared to the isotropic behaviour displayed by the highly symmetric spherical shell. Not surprisingly, in view of the increased proportion of the walls exposed to a parallel inducing field in its longitudinal orientation, the longitudinal apparent susceptibilities dominate the transverse values.

It is recalled that the standard drum has been chosen to have average parameter values. Since variations in these parameters are not uncommon in practice, it is useful to explore the individual influence of each on the apparent susceptibility. The spherical shell is useful in this connection since the effect of all parameters has been exposed in the above equations. However, the spherical shell is significantly more symmetrical than the drum, and so its use is somewhat limited for this reason.

It should first be noted that the apparent susceptibility as defined here depends only on the geometry of the body and is quite independent of scale. This behaviour has been noted previously in connection with the spherical shell. Consequently, if all dimensions of the drum (i.e. the radius r, height h and wall thickness t) are scaled by the same factor, the apparent susceptibilities remain exactly as shown in Fig. 5. In view of this behaviour, the only geometrical parame-

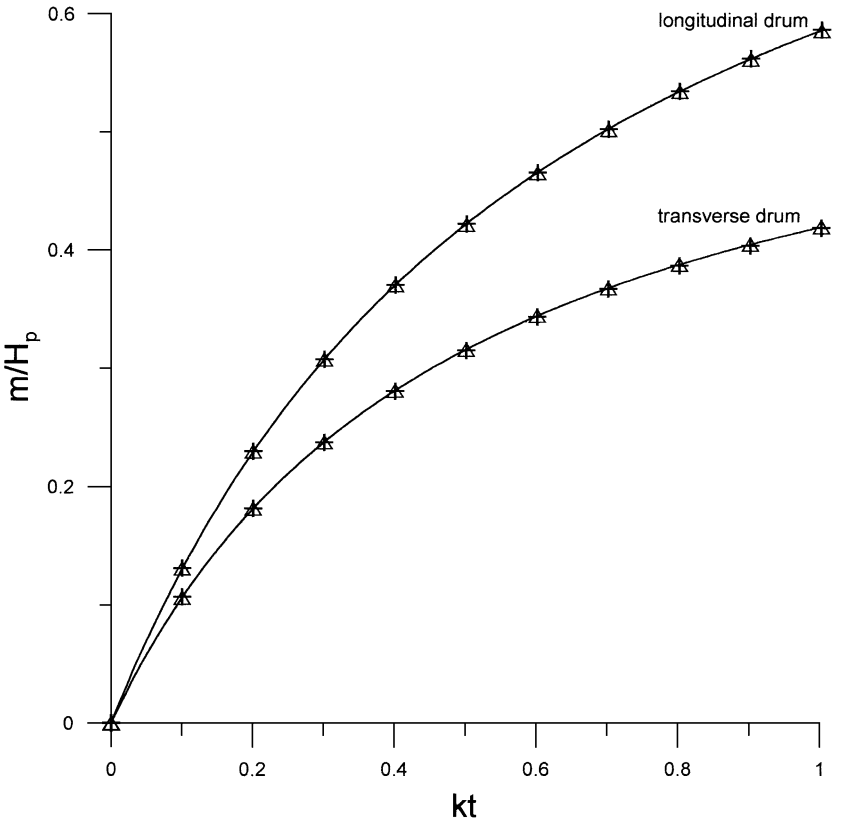

Fig. 6. Dipole moment as a function of susceptibility-thickness product for standard drums with wall thicknesses of 1.0 mm (continuous line), 0.5 mm (triangles) and 2.0 mm (crosses).

ters influencing the apparent susceptibility are the wall thickness ratio defined by t/h and the dimension ratio defined by r/h.

The effect of wall thickness can be easily anticipated. It is well known that the magnetic fields associated with thin, highly susceptible bodies depend on the susceptibility-thickness product (again, this behaviour has been noted in connection with the spherical shell). Fig. 6 confirms this in the case of a standard drum with wall thicknesses that span the expected range associated with these constructions. The continuous curves show the variation of the dipole moment with susceptibility-thickness product for the standard drum with a wall thickness of 1.0 mm in its two principal orientations. The data plotted with triangles are relevant to a drum with a wall thickness of 0.5 mm, while the crosses result from a significantly larger wall thickness of 2.0 mm. The agreement between the data is seen to be quite acceptable.

In view of this behaviour, it is a simple matter to extend the results for the standard drum as exposed in Fig. 5 (and expressed by Eq. (9)) to different wall thicknesses. Consider therefore the problem of finding the apparent susceptibilities of a drum with standard external dimensions, but with a wall thickness t' and a susceptibility k'. According to Fig. 6, this drum will produce the same dipole moment as a standard drum with wall thickness t and susceptibility k where

$$k = k't'/t$$

If Eq. (9) expressing the apparent susceptibility of a standard drum is denoted by

$$k_\alpha = f(k)$$

this dipole moment is given by

$$m = f(k't'/t)VH_p$$

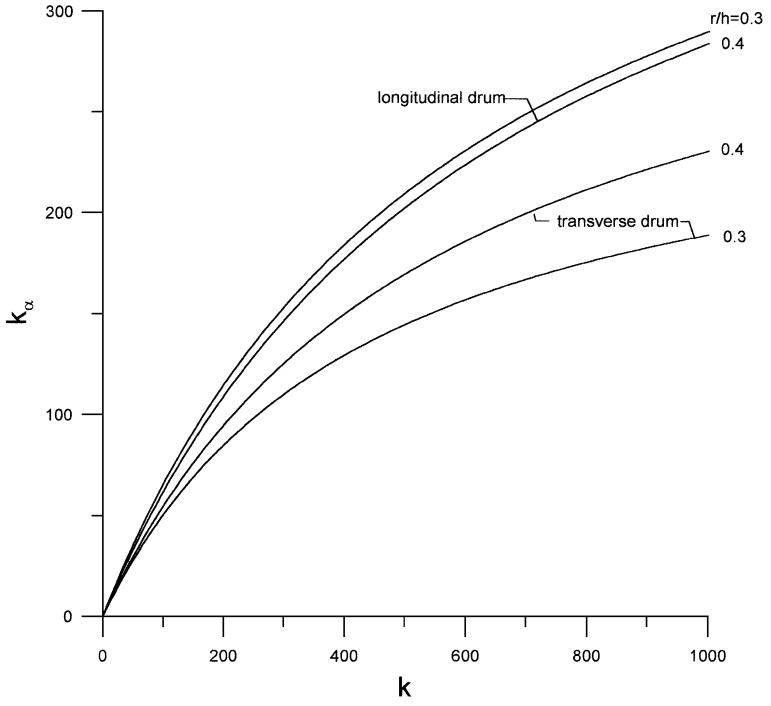

Fig. 7. Apparent susceptibility as a function of susceptibility for drums with dimension ratios of 0.3 and 0.4.

where V is the metal volume of the standard drum. It follows that the required apparent susceptibility is given by

$$k_\alpha = f(k't'/t)V/V' \tag{10}$$

where V' is the metal volume of the drum in question. Recalling that the external dimensions of the two drums are the same, it follows that for sufficiently thin walls, the metal volume of the drums can be expressed approximately as

$$V = At$$

and

$$V' = At'$$

where A is the surface area of the standard drum. Consequently, Eq. (10) can be more simply expressed in the form

$$k_\alpha = f(k't'/t)t/t'$$

The influence of the dimension ratio is not so easily accommodated. Because of its symmetry, the spherical shell has no analogous parameter and so provides no insight in this regard. It is recalled that the dimension ratio describes the shape of the drum, and this is one of the basic factors influencing the apparent susceptibility.

Fig. 7 shows the variation of apparent susceptibility with susceptibility for two drums with dimension ratios of 0.3 and 0.4. The dimension ratio of the standard drum at 0.3378 lies between these two extremes. Not surprisingly, the figure demonstrates a decreasing anisotropy in apparent susceptibilities associated with the more equidimensional drum. Also obvious is the fact that the transverse apparent susceptibilities are significantly more affected by the dimension ratio than the corresponding longitudinal values.

6. Approximate modelling of drum responses

Due to the complexities of more exact modelling procedures, it has become common to employ a variety of equivalent source modelling techniques

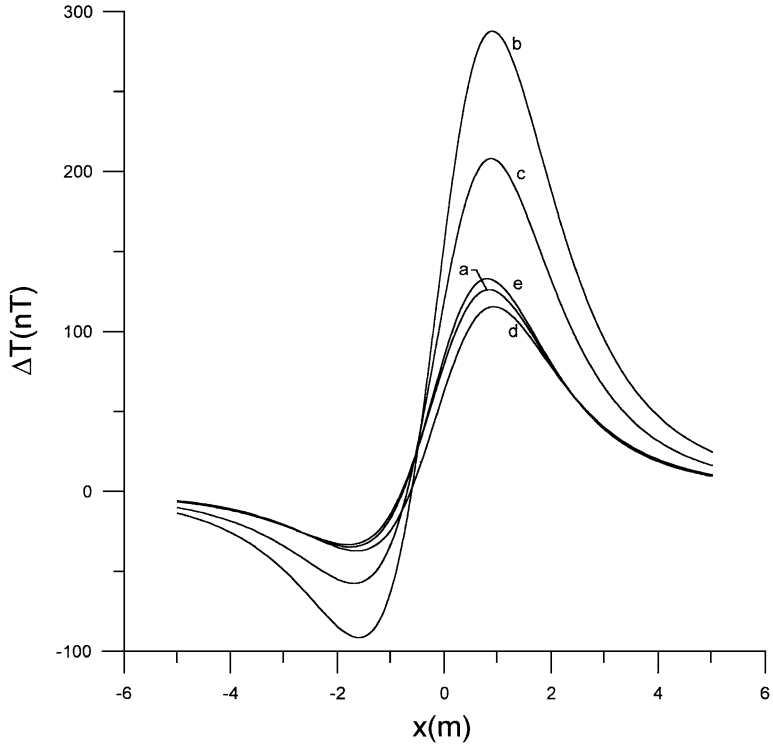

Fig. 8. Total field magnetic profile over a vertical standard drum buried 2 m below the sensor height computed by (a) the exact integral equation technique, (b) neglect of demagnetization effects, (c) use of local depolarizing factors, (d) use of the dipole moment due to an equivalent spherical shell and (e) use of a dipole moment computed from the longitudinal and transverse apparent susceptibilities of a standard drum.

for steel drums (e.g. Emerson et al., 1992; Ravat, 1996). In these techniques, the source body is represented by conveniently simple forms, e.g. cylindrical prisms and spheres magnetized in the direction of the earth's field. The results are found to predict the form of measured anomaly profiles satisfactorily. However, agreement with measured magnitudes is poor so that an equivalent susceptibility estimated by matching the measured and modelled responses is generally employed.

It is informative to review the application of these techniques in view of their computational efficiency compared to the exact integral equation method. Accordingly, Fig. 8 shows a north–south profile over a vertical standard steel drum computed by a variety of techniques. The figure shows the total field anomaly measured over a drum located 2 m below the sensor at a location in the southern hemisphere where the geomagnetic field has an amplitude of 50 000 nT, a declination of 0° and an inclination of -50°. Horizontal coordinates in the figure increase northwards.

Curve a shows the exact anomaly profile computed by Phillip's integral equation technique using 1440 planar surface elements. It displays a typical dipolar response with a total amplitude in the vicinity of 160 nT.

The first set of approximate profiles (curves b and c) result from approaches that recognize the true drum geometry (i.e. a hollow cylindrical prism), but approximate the magnetization by various simplifying assumptions. The profiles have been computed by specializing the general expression for the magnetic field due to the drum, i.e.

$$\mathbf{H}(\mathbf{r}) = \mathbf{H}_{\mathrm{p}}(\mathbf{r}) - \frac{1}{4\pi}\nabla \int\int_{V}\int \mathbf{M}(\mathbf{r}') \cdot \nabla' \frac{1}{|\mathbf{r}-\mathbf{r}'|}\,\mathrm{d}v'$$

to the case of an approximating N-sided plane polyhedral shell with wall thickness t. This results in

$$\mathbf{H}(\mathbf{r}) = \mathbf{H}_{\mathrm{p}}(\mathbf{r}) - \frac{t}{4\pi}\sum_{i=1}^{N}\nabla \times \left[M_{\mathrm{n}i}\int\int_{\Delta S_i} \hat{\mathbf{n}}\cdot\nabla' \frac{1}{|\mathbf{r}-\mathbf{r}'|}\mathrm{d}s' + M_{\mathrm{l}i}\sum_{j=1}^{N_i}\oint_{\Delta C_{ij}} \frac{\hat{\boldsymbol{l}}\cdot\hat{\boldsymbol{m}}_{ij}}{|\mathbf{r}-\mathbf{r}'|}\mathrm{d}c' \right] \quad (11)$$

where ΔC_{ij} is the jth edge of the ith polygonal face with median surface ΔS_i. $M_{\mathrm{n}i}$ and $M_{\mathrm{l}i}$ are the normal and longitudinal components of the magnetization in the wall of the ith face (Eskola et al., 1993). Eq. (11) is easily evaluated by identifying the first integral term as the field due to a uniform double layer on the plane polygonal surface ΔS_I, and the second as the field due to a uniform line source on the straight edge ΔC_{ij}.

Curve b is the result of assuming that the secondary magnetic field is negligible compared to the primary component so that the magnetization is given by

$$\mathbf{M} = k\mathbf{H}_{\mathrm{p}}$$

While the form of this curve reasonably approximates that of the true response, the true amplitude is seen to be grossly overestimated. This is understandable bearing in mind that the above assumption neglects demagnetization completely. While this approach is used here with a polyhedral shell model of the standard drum, it can also be implemented by differencing the responses due to two solid cylindrical prisms with dimensions equal to those of the inside and outside of the drum (Ravat,1996).

Curve c results from an attempt to account for demagnetization. It assumes that the local demagnetizing fields associated with a planar polygonal sheet of the hollow polyhedron are equivalent to that of an infinite sheet with zero depolarization factor in the longitudinal direction and unit depolarization factor in the normal direction. Accordingly, the components of the magnetization in the directions normal and parallel to the face are assumed to be given by

$$\mathbf{M}_{\mathrm{n}} = \frac{k}{1+k}\mathbf{H}_{\mathrm{pn}}$$

and

$$\mathbf{M}_{\mathrm{l}} = k\mathbf{H}_{\mathrm{pl}}$$

where $\mathbf{H}_{\mathrm{pn}}$ and $\mathbf{H}_{\mathrm{pl}}$ are corresponding components of the primary magnetic field. Again the form of the resulting profile (curve c) is seen to provide a good indication of the shape of the true profile but with the amplitude remaining excessively large.

The next set of profiles (curves d and e) results from representing the magnetic effect of the drum by an equivalent dipole. Accordingly, the anomalous magnetic field is simply given by

$$\mathbf{H}(\mathrm{r}) = -\nabla\left(\frac{1}{4\pi}\mathbf{m}\cdot\nabla'\frac{1}{|\mathbf{r}-\mathbf{r}'|}\right)$$

where $\mathbf{r}'$ is the position vector of the dipole with moment $\mathbf{m}$ located at the centroid of the drum.

Curve d is the result of approximating the dipole moment by that of a thin spherical shell with equal surface area and wall thickness, i.e. a shell with an equal metal volume to the drum. It is seen to provide a much improved fit to the theoretical profile than previous approximations albeit with a somewhat reduced amplitude.

Concerning the magnitude of the anomaly as seen on curve d, Fig. 5 shows that in a purely longitudinal primary field, the dipole moment of a standard drum is substantially larger than that produced by an equivalent spherical shell. Conversely, in a purely transverse field, the dipole moment of the drum is correspondingly smaller than that produced by the shell. It follows that the agreeable fit of curve d to the true profile in the present case is the fortuitous result of approximately equal longitudinal and transverse components of the primary field. Indeed, the noticeable underestimation of the anomaly magnitude of curve d reflects the fact that in the present situation, the drum is exposed to a somewhat larger component of the primary field in the longitudinal direction than in the transverse direction.

Finally, curve e is the result of using the longitudinal and transverse apparent susceptibilities computed for the standard drum in the last section. The longitudinal and transverse components of the equivalent dipole moment are therefore given by

$$\mathbf{m}_{\mathrm{l}} = \mathrm{k}_{\alpha\mathrm{l}}\mathbf{H}_{\mathrm{pl}}V$$

and

$$\mathbf{m}_t = k_{\alpha t}\mathbf{H}_{pt}V$$

where V is the volume of metal. $k_{\alpha l}$ and $k_{\alpha t}$ are the longitudinal and transverse apparent susceptibilities whose values are taken from Fig. 5.

This last curve shows the best fit to the true response profile of all the approximations in terms of both the amplitude and the shape. However, the amplitude is seen to be somewhat underestimated—a result of higher multipoles in the response behaviour that are not accommodated by the apparent susceptibilities. Since the fields due to these multipoles attenuate much more rapidly than the dipolar effect, the present approximation can be expected to rapidly approach the true profile with increasing separation of the sensor and source body. This condition is clearly evident on the southern and northern thirds of the profile, where curves a and e show close agreement. It is also worth noting that in contrast to the spherical shell approximation, the agreeable correspondence between curve e and the true profile can be expected for all orientations of the drum and primary field.

7. Conclusions

While all the approximations considered in the present discussion reasonably predict the form of the total field magnetic profiles measured over a standard steel drum, only those based on an equivalent spherical shell and on the numerically computed apparent susceptibilities predict the amplitudes with any accuracy.

The general magnetic characteristics of a standard drum are reasonably approximated by those of a thin spherical shell with equal susceptibility, wall thickness and metal content. For modelling applications, where the drum orientation is unknown, this is probably the most useful approximate model for drum responses.

However, the spherical shell fails to account for the significant anisotropy in apparent susceptibility displayed by the standard drum. Where the orientation of the drum is known, the use of the individual longitudinal and transverse apparent susceptibilities results in a significant improvement in the approximate modelling of drum responses.

Finally, it should be noted that while the above discussion specifically concerns 205-l steel drums, the results are directly applicable to drums with different capacity, provided the geometry, as defined by the thickness and dimension ratios, remains the same as those considered here. Typical 60- and 25-l closed head drums currently manufactured in Australia qualify in this regard. Drums of smaller capacity, however, generally have significantly larger dimension ratios.

References

Barrows, L., Rocchio, J.E., 1990. Magnetic surveying for buried metallic objects. Ground Water Monitoring Review 10, 204–211.

Emerson, D.W., Reid, J.E., Clark, D.A., Hallett, M.S.C., Manning, P.B., 1992. The geophysical responses of buried drums-field tests in weathered Hawkesbury Sandstone, Sydney Basin, NSW. Exploration Geophysics 23, 589–617.

Eskola, L., 1992. Geophysical Interpretation Using Integral Equations. Chapman & Hall, London.

Eskola, L., Soininen, H., Oksama, M., 1989. Modelling of resistivity and IP anomalies of a thin conductor with an integral equation. Geoexploration 26, 95–104.

Eskola, L., Jokinen, T., Soininen, H., Tervo, T., 1993. Some remarks on static field thin sheet models. Journal of Applied Geophysics 30, 229–234.

Eskola, L., Puranen, R., Soininen, H., 1999. Measurement of magnetic properties of steel sheets. Geophysical Prospecting 47, 593–602.

Furness, P., 1999. A versatile integral equation method for magnetic modelling. Journal of Applied Geophysics 41, 345–357.

Jackson, J.D., 1975. Classical Electrodynamics. Wiley, New York.

Nabigian, M.N., Oppliger, G.L., Edwards, R.N., Lo, B.B.H., Cheesman, S.J., 1984. Cross-hole magnetometric resistivity (MMR). Geophysics 49, 1313–1326.

Phillips, H.B., 1934. Effect of surface discontinuity on the distribution of potential. Journal of Mathematics and Physics 13, 261–267.

Ravat, D., 1996. Magnetic properties of unrusted steel drums from laboratory and field-magnetic measurements. Geophysics 61, 1325–1335.

Traynin, P., Hansen, R.O., 1993. Magnetic modeling for highly permeable bodies with remanent magnetization. 63rd Annual International Meeting of the Society of Exploration Geophysicists. Expanded Abstracts, pp. 410–413.

Van Bladel, J., 1985. Electromagnetic Fields Hemisphere Publishing, New York.